



Astrometric Observations of NEA 1998 HH49 Using the Daocheng 50 cm Telescope

Huan Xu^{1,2}, Xiang-Ming Cheng^{1,2,3,4} , Yi-Gong Zhang⁵, Teng-Fei Song¹, Zhen-Jun Zhang⁶, and Qing-Yu Peng^{7,8}

¹Yunnan Observatories, Chinese Academy of Sciences, Kunming 650216, China; cxm@ynao.ac.cn

²University of Chinese Academy of Sciences, Beijing 100049, China

³Key Laboratory of the Structure and Evolution of Celestial Objects, Chinese Academy of Sciences, Kunming 650216, China

⁴Engineering Laboratory on Applied Astronomical Technology of Yunnan, Kunming 650216, China

⁵School of Information Engineering, Kunming University, Kunming 650214, China

⁶School of Computer Science and Information Engineering, Anyang Institute of Technology, Anyang 455000, China

⁷Department of Computer Science, Jinan University, Guangzhou 510632, China

⁸Sino-French Joint Laboratory for Astrometry, Dynamics and Space Science, Jinan University, Guangzhou 510632, China

Received 2024 March 6; revised 2024 May 13; accepted 2024 May 13; published 2024 July 8

Abstract

This study details an astrometric observation campaign of the Near-Earth Asteroid 1998 HH49, conducted with the aim of refining our understanding of its physical characteristics. Utilizing the 50 cm telescope located at the Wumingshan Mountain in Daocheng, Sichuan, images were obtained over four nights, from 2023 October 19 to October 22. These observations were processed using Astrometrica software, facilitating the precise determination of the asteroid's position. The observational results were compared with the ephemerides from three distinct sources to verify accuracy: the Jet Propulsion Laboratory (JPL) Horizons System, the Institut de Mécanique Céleste et de Calcul des Éphémérides (IMCCE) Miriade, and the Near-Earth Objects Dynamic Site (NEODYs-2). When compared with the JPL ephemeris, a mean observed-minus-calculated (*O-C*) result of $0''.07$ in the R.A. direction and $-0''.35$ in the decl. direction was yielded. Furthermore, the comparison with the IMCCE ephemeris yielded mean *O-C* results of $0''.08$ in the R.A. direction and $-0''.06$ in the decl. direction. The comparison with the NEODYs-2 ephemeris yielded the mean *O-C* results of $0''.06$ in R.A. and $-0''.49$ in decl. direction. The study's findings demonstrate a general consistency between the observed data and the ephemeris predictions, with minor discrepancies observed across the data sets. Notably, both the JPL and NEODYs-2 ephemerides show that the residuals in the decl. direction exceed those in the R.A. direction. The disparities may result from atmospheric differential color refraction, ephemeris discrepancies, observational errors, and other factors. Additionally, it is worth noting that further investigation is required due to the potential influence of additional factors. Overall, the Daocheng 50 cm Telescope exhibits the ability to conduct high-precision positional measurements.

Key words: astrometry – ephemerides – time

1. Introduction

The execution of high-precision astrometry for Near-Earth Objects (NEOs) not only substantially contributes to pivotal scientific inquiries regarding the solar system's genesis and progression but also fortifies global preparedness against the contingency of NEO impacts. The subject of NEO mitigation is integral to strategic advancements within the ambit of China's scientific endeavors, marking a significant directive in the "14th Five-Year Plan." Commencing in 2021, China has embarked on formulating a long-term strategy for NEO impact risk management, with ambitions to orchestrate kinetic impact deflection trials on selected near-Earth asteroids within this timeframe. The basis for accurate orbital determination of NEOs rests on the acquisition of precise epochal positions.

The measurement and tracking of near-Earth asteroids (NEAs) utilize a diverse range of space-based and ground-

based technologies, each with distinct capabilities and limitations. Space-based technologies, exemplified by missions such as Near-Earth Object Wide-field Infrared Survey Explorer (NEOWISE) (Mainzer et al. 2011), employ infrared sensors to detect the thermal emissions of asteroids. This method is less affected by daylight and atmospheric conditions, facilitating continuous monitoring. The recently launched Near-Earth Object Surveillance Mission (NEOSM, later renamed NEO Surveyor) extends these capabilities by providing more comprehensive coverage and enhanced detection sensitivity. However, space missions are considerably more expensive and involve complex logistics and extended preparation times. Following space-based systems, ground-based techniques play a pivotal role in the comprehensive observation of NEAs. These techniques predominantly involve radar measurements and the utilization of optical telescopes. Radar technology, such

as that used by NASA's Goldstone Solar System Radar, provides precise determinations of an asteroid's location, shape, velocity, and even facilitates imaging of asteroid surfaces. However, the effectiveness of radar is limited by range capabilities and necessitates that asteroids be relatively close to Earth for optimal functionality. In addition to radar measurements, ground-based optical telescopes are instrumental in discovering new asteroids. Systems like Panoramic Survey Telescope and Rapid Response System (Pan-STARRS) (Kaiser et al. 2002), which employs wide-field cameras to detect and track asteroids against stellar backgrounds, significantly contribute to the field of discovery and monitoring of celestial measurements. Although large ground-based telescopes offer superior observational capabilities compared to smaller apertures, their number is limited and their available observing time is often heavily booked. Additionally, the vast quantity of NEAs means that relying solely on large telescopes is insufficient for observing all such targets. These targets typically require long follow-up observation history and extensive follow-up observations to derive precise astrometric coordinates. A critical bottleneck in conducting observations of these targets is the constriction of appropriate observational windows, which demands a coordinated effort across a global network of telescopes capable of effective tracking. In particular, the dynamic nature of these objects, influenced by gravitational interactions with planets and the Sun, as well as non-gravitational forces such as the Yarkovsky effect, makes predicting their long-term trajectories a complex task (Bottke et al. 2006; Ivezić et al. 2007). Smaller telescopes are important supplementary equipment for observing asteroids. Consequently, smaller-aperture telescopes become essential tools for such observations. Thus, maximizing the astrometric observational utility of China's existing and forthcoming observatory infrastructures is of paramount importance for enhancing NEO research and defense mechanisms.

Considerable scholarly attention has been allocated to the study of Potentially Hazardous Asteroids (PHAs). These research efforts are dedicated to conducting astrometric observations of NEOs including PHAs to obtain high-precision epoch positions (Wang et al. 2014; Zhang et al. 2015; Perna et al. 2016; Zhang et al. 2019). This paper focuses on the astrometric study of 1998 HH49, a PHA discovered on 1998 April 20, by the Lincoln Near-Earth Asteroid Research (LINEAR) (Stokes et al. 2000). According to the Minor Planet Center (MPC) database, the NEA 1998 HH49 was discovered on 1998 April 24, by Spacewatch survey (MPC code 691). Minor Planet Electronic Circulars (MPECs) made a double announcement about this target (Gehrels et al. 1998; Veillet et al. 2000). The asteroid is classified as a PHA because of its orbit, which allows for close approaches to Earth, and its estimated size of 650 m by 190 m. 1998 HH49 orbits the Sun with a semimajor axis of 1.22 astronomical units (au), an orbital period of approximately 2.8 yr, an absolute magnitude

of 21.4, and a rotational period of about 2.7 hr. The close approaches of this asteroid to Earth could pose a significant regional threat, with its substantial mass estimated at 50 million tons and specific orbital characteristics, which include a close approach to Earth within 60–78 times the planet's diameter. These attributes coupled with its potential energy release, equivalent to multiple hydrogen bombs, have led to its selection for discussion as a possible "Asteroid Weapon" in strategic defense scenarios (Lunan 2014). These characteristics highlight the necessity of precise astrometric monitoring to refine our understanding of its trajectory and physical properties, thereby assessing the potential impact risk it poses. This study presents the outcomes of an astrometric observation experiment conducted on 1998 HH49, aiming to improve our knowledge of its location.

The Wumingshan Mountain site, located in Daocheng, Sichuan at an altitude of 4700 ~ 4800 m with coordinates of longitude 100°06'E and latitude 29°06'N, is recognized by Yunnan Observatories for its favorable conditions for astronomical observations (Song et al. 2020; 2021). The site features an average annual cloud cover of less than 50%, up to 270 clear nights per year as defined by astronomical standards, a middle night seeing of 0".9, air integral water vapor content of 2.5 mm, relative humidity below 60%, and an average wind speed of less than 5 m s⁻¹ (Liu et al. 2018). Here, the Daocheng 50 cm Telescope is accompanied by a 6.3 m spherical dome with a 1.2 m wide skylight enabling 360° rotation. See Figure 1 for an image of the telescope and observation room. To address the challenges of conducting observations at high altitudes and to enable remote, automated observations with the 50 cm optical telescope at the Wumingshan site, Zhang Guanjun et al. embarked on significant modifications. They utilized the Modbus/TCP protocol to integrate a Programmable Logic Controller (PLC), achieving automated control over the dome (Zhang et al. 2020). This strategic implementation is pivotal for remote observations, marking a substantial enhancement in the telescope's operational capabilities and providing a reference model for automation in mid-size astronomical observation systems.

The core of this paper is structured as follows: Section 2 outlines a detailed account of a four-night observational endeavor at the Wumingshan Mountain in Daocheng, Sichuan, utilizing the 50 cm telescope to acquire images containing moving targets. Section 3 progresses into data processing, wherein the observed positions of the asteroid are meticulously compared with the ephemeris from the Jet Propulsion Laboratory (JPL), Institut de Mécanique Céleste et de Calcul des Éphémérides (IMCCE), and Near-Earth Objects Dynamic Site (NEODyS-2). Section 4 analyzes the astrometric measurements obtained. Section 5 delves into the discussion of factors that could potentially influence these measurements. The final section of the paper provides a summary. This synthesis not



Figure 1. Daocheng 50 cm Telescope (Left) and Observation Room (Right).

Table 1
Observational Data for Asteroid 1998 HH49

Date	Magnitude	Sky Coordinates		$dR.A./dt \times \cos(\text{Decl.})$ (" minute ⁻¹)	$d(\text{Decl.})/dt$ (" minute ⁻¹)	Distance to Earth (au)
		Azi.	Alt.			
2023-10-19	14.1	96	+35~55	11.99	13.57	0.022
2023-10-20	14.7	89	+34~54	6.52	7.31	0.030
2023-10-21	15.2	86	+34~54	4.04	4.52	0.039
2023-10-22	15.6	84	+40~43	2.70	3.05	0.047

Note. Values for $dRA/dt \times \cos(\text{decl.})$ and $d(\text{decl.})/dt$ are average rates during observation. Values for Azi. are taken at the middle observation time.

only advances our knowledge in PHAs but also plays a pivotal role in advancing our understanding of NEOs.

2. Observations

We conducted the astrometric observations of 1998 HH49 using a 50 cm telescope equipped with a CCD camera that had a resolution of 2048×2048 pixels and a focal length of 3454 mm at the Wumingshan Mountain in Daocheng, Sichuan. These observations were carried out over the course of four nights, from 2023 October 19th to October 22nd. The target in the images exhibits an approximate signal-to-noise ratio (S/N) of about 30. Partial information about the targets observed during these four nights is listed in Table 1. Details regarding the telescope and CCD detectors are presented in Table 2. A typical image of the observational targets is shown in Figure 2.

The astrometric observations of NEA 1998 HH49 were conducted using the J2000.0 epoch as the reference time. This choice aligns with standard astronomical practices for ensuring consistency in celestial coordinates across different observational data sets. The coordinate system employed was the International Celestial Reference System (ICRS), an ideal

Table 2
Specifications of the 50 cm Telescope and CCD Detector

Focal Length	CCD FOV	Size of Pixel	CCD Array
3454 mm	21' 8 × 21' 8	11 μm × 11 μm	2048 × 2048

framework that uses the positions of distant extragalactic sources for its practical realization in the International Celestial Reference Frame (ICRF). This system provides a stable framework for reporting celestial positions. The acquisition of flat-field images was performed during twilight to mitigate potential image brightness discrepancies caused by variations in pixel sensitivity and optical system flaws. Each evening, approximately ten flat-field frames were captured to ensure thorough calibration. Dark-frame images were acquired by utilizing identical exposure times as those used for capturing the target object. This procedure aimed to correct thermal noise resulting from extended exposure durations. We obtained images of the asteroid in the Clear filter with an exposure time that varied each night depending on the asteroid's apparent

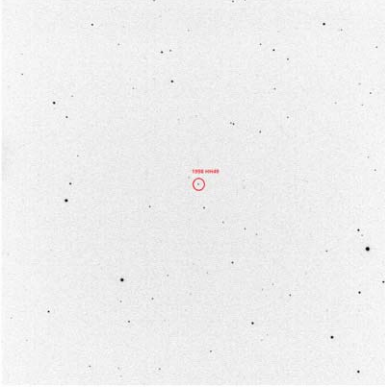


Figure 2. CCD image of 1998 HH49 captured on 2023 October 21, with an exposure duration of 6 s.

motion: 2, 4, 6, and 8 s per frame. The filter was used to capture up to 100 frames on some nights. The resulting images had dimensions of 2048×2048 pixels each. We processed the images using standard astrometric techniques to determine the precise position of the asteroid relative to nearby stars. These measurements may potentially be used for orbital calculations. The specific observation information can be found in Table 3.

3. Data Reduction

3.1. Target Position

To ensure the quality of the astrometric analysis, images with poor fits, such as those affected by cloud cover, are excluded. The valid images are processed using the astrometric software Astrometrica (Raab 2012) for flat-field and dark-frame corrections, as well as for determining the topocentric astrometric position in equatorial coordinates of the target. After selecting the Gaia Data Release 2 (DR2) star catalog (Gaia Collaboration et al. 2018) and a QUADRATIC FIT model for plate solution, the target is manually identified and marked to generate an output text file with the asteroid's measured position.

3.2. O-C Results

Ephemerides for the target asteroid were obtained from the JPL, IMCCE, and NEODYs-2 databases. Due to the asteroid's rapid motion, the JPL ephemeris precisely matched our observation timings. The ephemeris from IMCCE and NEODYs-2 both utilize a one-minute time interval. The one-minute time intervals were subsequently interpolated using quadratic interpolation to obtain the values at the exact moments of our observations. For IMCCE, tests across intervals from 0.01 s to 1 minute confirmed interpolation errors remained below 1 milliarcsecond, validating the use of one-minute intervals. NEODYs-2 data, with their fixed one-minute interval, were used directly without additional testing. The

Table 3
Consolidated Observational Information for 1998 HH49

Date	Filter	Exposure Time (s)	Valid Frames
2023-10-19	C	2	99
2023-10-20	C	4	116
2023-10-21	C	6	116
2023-10-22	C	8	93

variations in target positions among different ephemerides primarily stem from the differing orbital theory underlying each ephemeris and the distinct data sets used for orbital fitting. The JPL case primarily utilizes its own Development Ephemeris (DE) series, such as DE440 and DE441, which are sophisticated models based on general relativity for high precision ephemerides. In contrast, the IMCCE uses planetary theory like INPOP19a for integrating both Newtonian dynamics and relativistic corrections into their calculations. NEODYs-2, focusing on NEOs, employs numerical integration methods to track and predict asteroid trajectories effectively, catering specifically to the dynamic nature of these bodies. Each of these models is continuously refined and updated to incorporate the latest observational data, ensuring accuracy in their respective domains. The following Table 4 summarizes the orbital parameters and epoch used by mentioned ephemeris services.

Quadratic interpolation was applied to the ephemerides to derive the astrometric positions for the precise moments of our observations. This procedure simplified the process of comparing observed (*O*) and calculated (*C*) positions, ultimately leading to the derivation of observed-minus-calculated (*O-C*) discrepancies. Additionally, all our calculations are based on topocentric celestial positions. To enhance the accuracy of our analysis, outlier points were efficiently removed by applying the 3σ rule, resulting in more accurate *O-C* values, unaffected by outlier data point interference. The *O-C* results from every day are shown in Table 5. Figure 3 presents the *O-C* results in the R.A. and decl. directions over four days, comparing the ephemerides from the JPL, IMCCE, and NEODYs-2 cases. The reason for the dispersion changes in the *O-C* in Figure 3 is significantly related to the target's motion speed. This can be easily observed by comparing the residual plots here with the motion speeds listed in Table 1.

4. Results Analysis

Calculations based on the *O-C* results from the figures and tables reveal that the NEODYs-2 ephemeris shows the mean *O-C* value of $0''.06$ in R.A. and $-0''.49$ in decl., the JPL ephemeris presents the *O-C* values of $0''.07$ in R.A. and $-0''.35$ in decl., and the IMCCE ephemeris yields the mean *O-C* values of $0''.08$ in R.A. and $-0''.06$ in decl. It is evident that the *O-C* residuals are consistent across the three sources: NEODYs-2, JPL, and

Table 4
Orbital Elements of Asteroid 1998 HH49 from Various Sources

Orbital Element	JPL	IMCCE	NEODYs-2
Semimajor Axis (a)/au	1.551	1.551	1.558
Eccentricity (e)	0.502	0.502	0.503
Inclination (i)/deg	8.419	8.419	8.429
Longitude of Ascending Node (Ω)/deg	23.473	23.484	23.458
Argument of Periapsis (ω)/deg	287.909	287.884	288.259
Mean Anomaly (M)/deg	7.185	267.734	108.399
Epoch	2460200.5 (2023-Sep-13.0) TDB	2021-03-27 TDT	60400.0 MJD

Table 5
Mean and Standard Deviation of the ($O-C$) Residuals for 1998 HH49

Date	R.A. ($O-C$)(")			Decl. ($O-C$)(")		
	JPL	IMCCE	NEODYs-2	JPL	IMCCE	NEODYs-2
10–19	0.22 ± 0.27	0.24 ± 0.27	0.20 ± 0.26	-0.41 ± 0.29	0.10 ± 0.29	-0.74 ± 0.44
10–20	0.11 ± 0.17	0.12 ± 0.17	0.10 ± 0.17	-0.45 ± 0.18	-0.15 ± 0.18	-0.56 ± 0.22
10–21	0.06 ± 0.12	0.06 ± 0.12	0.05 ± 0.12	-0.37 ± 0.14	-0.16 ± 0.14	-0.46 ± 0.16
10–22	-0.11 ± 0.16	-0.11 ± 0.16	-0.12 ± 0.16	-0.16 ± 0.18	-0.01 ± 0.18	-0.21 ± 0.18
Overall Four-Day	0.07 ± 0.14	0.08 ± 0.15	0.06 ± 0.13	-0.35 ± 0.13	-0.06 ± 0.12	-0.49 ± 0.22

IMCCE. The $O-C$ values derived from the JPL and NEODYs-2 ephemerides in both R.A. and decl. directions reveal a finding: the $O-C$ residuals in the R.A. direction are significantly better than in the decl. direction. While the IMCCE ephemeris does not exhibit a significant discrepancy, the $O-C$ values on the first day are noticeably larger, which could be attributed to the greater speed on that day. In addition, the asteroid's speed is slightly higher in the decl. direction compared to the R.A. direction. Although both ephemerides show smaller $O-C$ values in the R.A. direction than in the decl. direction, the small difference in speed between the two directions suggests that the impact of the asteroid's motion on the inconsistency in $O-C$ values across R.A. and decl. can be considered negligible. Further investigation is required to understand the underlying causes of the observed variations in $O-C$ residuals between the two directions.

5. Discussion

Through the analysis of the target's $O-C$ results, the following discrepancies are identified: the differences in $O-C$ values brought about by various ephemerides and the variation in $O-C$ values between the R.A. and decl. directions as observed in the JPL and NEODYs-2 ephemerides. Referencing Brumberg (2017), a brief analysis of the results of this paper is conducted:

- (1) *Observational Errors*: These can arise from several sources, including instrument calibration, data processing, and human error. The optical and tracking systems of the 50 cm telescope were meticulously calibrated, and

the exposure time for the observations was less than 10 s, resulting in no significant defects in the observed images. Data processing employed Astrometrica software, significantly reducing the impact of data handling and human error. Through the analysis of multiple reference background stars at different times using two-dimensional Gaussian centroiding methods calculated, the standard deviation for R.A. was found to average approximately $0''.064$, and for decl., approximately $0''.067$. These observed error values consistently show low error, indicating high stability and reliability in the observational methods and a slightly more pronounced impact on decl. than on R.A., though the overall effect remains minor.

- (2) *Geometric Distortions in CCD Imaging*: CCD cameras are widely used in astrometry but can introduce geometric distortions due to pixel irregularities, optical misalignments, and thermal effects. Some research (Peng & Tu 2011; Peng et al. 2012) discusses methods for correcting these distortions, which is crucial for reducing errors in astrometric measurements. In all observed images within this paper, the asteroid 1998 HH49 is positioned near the center of the field of view (FOV) to minimize the impact of field distortion. A detailed correction of field astrometric distortion will contribute to further enhancing the accuracy in the R.A. direction of observational results. This also highlights a critical area for future research: reducing errors in celestial measurements by developing and applying distortion models.

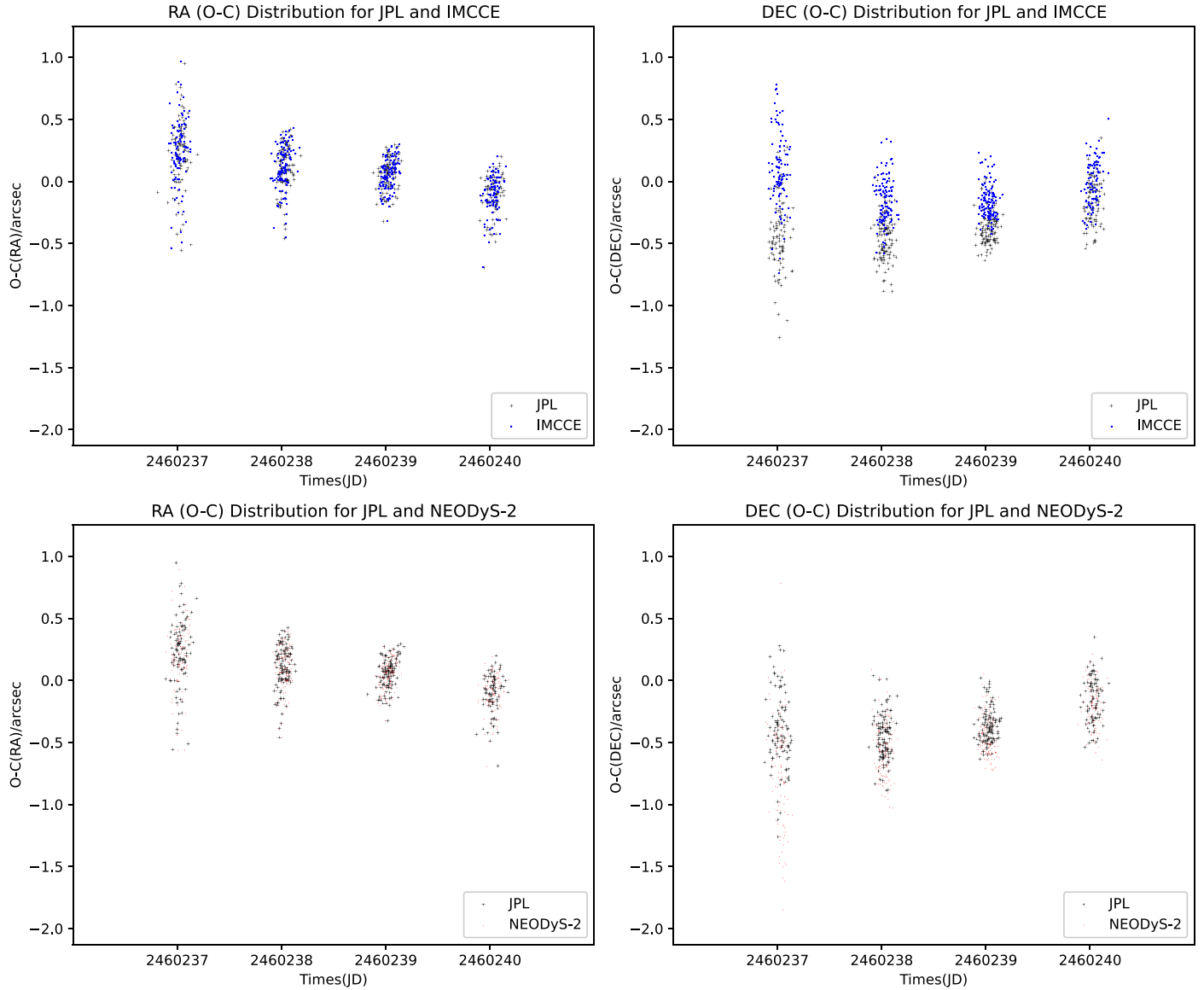


Figure 3. Comparison of $O-C$ from the JPL, IMCCE, and NEODYs-2 ephemerides. The upper row shows JPL versus IMCCE, with R.A. on the left and decl. on the right. The lower row displays JPL versus NEODYs-2, with R.A. on the left and decl. on the right.

(3) *Deviation of photocenter:* The non-uniform geometry of an asteroid can influence the reflection of its light, thereby impacting its perceived location. Thus understanding and modeling the object's shape can lead to more accurate predictions of its apparent motion and position, given that the size of 1998 HH49 is approximately 650 m. According to Table 1, the distance between the target and Earth is approximately 0.03 au. The angle between the Earth and the Sun with the target at the center is approximately $19^{\circ}43'$. Referencing the method for calculating the brightness center deviation described in Lindegren (1977), the calculated offset of the brightness

center is 47.84 m. We can determine that the astrometric position deviation caused is approximately $0''.002$. Therefore, the impact of the photocenter deviation on astrometric processing results is negligible.

(4) *Atmospheric Refraction:* This phenomenon can result in the bending of light from celestial objects as it passes through the Earth's atmosphere, leading to an altered apparent position in the sky. Atmospheric refraction causes the apparent position of objects to shift, which depends on their elevation in the sky. This shift affects both the R.A. and decl. coordinates, altering how celestial objects are observed from Earth. The high-order constant

model includes the effects of atmospheric refraction, thus the impact of atmospheric refraction does not need to be considered in this paper.

- (5) *Differential Color Refraction*: The phenomenon of Dispersion and Color Refraction (DCR) occurs when light of varying wavelengths undergoes differential refraction in the atmosphere due to variations in refractive indices. This is attributed to the wavelength-dependent nature of atmospheric refractive index, wherein shorter wavelengths (e.g., blue light) experience greater refraction compared to longer wavelengths (e.g., red light) (Stone 2002). Research conducted by Guo and his team, along with Lin and associates, has significantly advanced our understanding of DCR (Lin et al. 2020; Guo et al. 2023). A fundamental model of DCR typically assumes that DCR is primarily determined by the color index of the celestial body and the zenith distance of observation. Below is a simplified method for calculating DCR

$$\text{DCR} = k \cdot \tan(Z) \cdot (CI).$$

k is a coefficient that reflects the degree of refraction per unit color index and at the zenith distance of 45 degrees. This coefficient needs to be empirically determined based on observational data or theoretical predictions. In this paper, we utilize a k -value of 0.1 as provided in Guo et al. (2023). Z is the zenith distance, the angle from the observer's zenith to the celestial object.

CI is the color index of the star, which quantifies the difference in magnitude between two photometric filters. In this paper, we follow the work of Zhai et al. (2024), setting the CI value to 0.85 (Zhai et al. 2024).

Using this model, calculation results based on the article range from $0''.06$ to $0''.13$. However, it is important to emphasize that accurate DCR values are influenced by a variety of factors including climate conditions (humidity, temperature), the elevation of the observation site, and the composition of the atmosphere, necessitating more complex models for computation, a point that future research will consider.

6. Conclusions

In this paper, we present an astrometric analysis of the NEA 1998 HH49, conducted using the 50 cm telescope at Wumingshan Mountain in Daocheng, Sichuan. The $O-C$ results showed a discrepancy from the JPL ephemeris of about $0''.07$ in R.A. and $-0''.35$ in the decl. direction. The IMCCE ephemeris was $0''.08$ in the R.A. direction and $-0''.06$ in the decl. direction. The NEODYs-2 ephemeris revealed the best results with discrepancies of $0''.08$ in the R.A. and $-0''.49$ in the decl. directions. This analysis highlights the variance in accuracy

between different ephemeris sources when applied to astrometric observations of NEAs. But overall, these results show that the observational data are consistent with the three ephemerides used in this study. The IMCCE ephemeris provides the closest match to our observed positions in both R.A. and decl. directions. The other two ephemerides exhibited disparities in both R.A. and decl., which could potentially be attributed to DCR influence, minor observational inaccuracies or variations in the orbital models employed by the ephemerides. Consequently, this matter necessitates further comprehensive investigation. Furthermore, it is essential to consider various factors such as the target's velocity, atmospheric refraction, observational errors, the celestial object's shape, DCR, and CCD geometric distortions to enhance the precision of astrometric results. Based on the observational research findings of this paper, the 50 cm telescope with favorable astronomical observation conditions at the Daocheng Wumingshan Mountain site is capable of supporting the high-precision astrometric measurement requirements for NEOs, offering important backing for China's endeavors in NEO defense and kinetic impact experiments.

Acknowledgments

We acknowledge the support from the staff at the 50 cm telescope administered in Daocheng Observatory. This study benefited from the precise ephemeris data provided by the Jet Propulsion Laboratory (JPL) and the Institut de Mécanique Céleste et de Calcul des Éphémérides (IMCCE), enhancing the accuracy of our astrometric analysis. Additionally, we are deeply thankful for the application of Astrometrica software for astrometric data processing, which significantly contributed to the success of our observations and data analysis. Additionally, this research has made use of data provided by the NEODYs-2 service, and we acknowledge their contribution with gratitude. This work was funded by the National Key R&D Program of China (grant No. 2022YFE0116800), the National Natural Science Foundation of China (NSFC, grant No. 12173085), and the West Light Foundation of The Chinese Academy of Sciences Key scientific research projects of colleges and universities in Henan Province (grant No. 23B16001).

ORCID iDs

Xiang-Ming Cheng  <https://orcid.org/0000-0002-0282-528X>

References

- Botke, J., William, F., Vokrouhlický, D., Rubincam, D. P., & Nesvorný, D. 2006, *AREPS*, 34, 157
- Brumberg, V. 2017, *Essential relativistic celestial mechanics* (Boca Raton, FL: CRC Press)
- Gaia Collaboration, Brown, A. G. A., Vallenari, A., et al. 2018, *A&A*, 616, A1
- Gehrels, T., Scotti, J. V., & Williams, G. V. 1998, *MPEC*, 1998-J08
- Guo, B. F., Peng, Q. Y., Fang, X. Q., & Lin, F. R. 2023, *MNRAS*, 525, 4999

- Ivezić, Ž., Tyson, J. A., Jurić, M., et al. 2007, in *Near Earth Objects, our Celestial Neighbors: Opportunity and Risk*, ed. G. B. Valsecchi, D. Vokrouhlický, & A. Milani, Vol. 236 (Cambridge: Cambridge Univ. Press), 353
- Kaiser, N., Aussel, H., Burke, B. E., et al. 2002, *Proc. SPIE*, 4836, 154
- Lin, F. R., Peng, Q. Y., & Zheng, Z. J. 2020, *MNRAS*, 498, 258
- Lindgren, L. 1977, *A&A*, 57, 55
- Liu, Y., Li, X. B., Zhang, X. F., et al. 2018, *Proc. SPIE*, 10704, 784
- Lunan, D. 2014, *Incoming Asteroid!: What Could We Do About It?*, 109 (New York: Springer)
- Mainzer, A., Bauer, J., Grav, T., et al. 2011, *ApJ*, 731, 53
- Peng, Q. Y., & Tu, B. 2011, *SSPMA*, 41, 1126
- Peng, Q. Y., Vienne, A., Zhang, Q. F., et al. 2012, *AJ*, 144, 170
- Perna, D., Dotto, E., Ieva, S., et al. 2016, *AJ*, 151, 11
- Raab, H. 2012, *Astrometrica* software
- Song, T.-F., Liu, Y., Wang, J.-X., et al. 2020, *RAA*, 20, 85
- Song, T. F., Liu, Y., Cai, Z. C., et al. 2021, *MNRAS*, 505, 3070
- Stokes, G. H., Evans, J. B., Viggh, H. E. M., Shelly, F. C., & Pearce, E. C. 2000, *Icarus*, 148, 21
- Stone, R. C. 2002, *PASP*, 114, 1070
- Veillet, C., Shapiro, A., & Williams, G. V. 2000, MPEC, 2000–Y39
- Wang, X. W., Cao, J., & Peng, Q. Y. 2014, *AR&T*, 11, 34
- Zhai, C. X., Shao, M., Saini, N., et al. 2024, *PASP*, 136, 034401
- Zhang, G. J., Song, T. F., Cheng, X. M., Wang, J. X., & Zhang, Y. G. 2020, *AR&T*, 17, 548
- Zhang, X.-L., Yu, Y., Wang, X.-L., et al. 2015, *RAA*, 15, 435
- Zhang, Z.-J., Zhang, Y.-G., Cheng, X.-M., Wang, J.-C., & Su, J. 2019, *RAA*, 19, 071